HHS Public Access

Author manuscript

Nat Immunol. Author manuscript; available in PMC 2021 June 01.

Published in final edited form as:

Nat Immunol. 2020 June ; 21(6): 615–625. doi:10.1038/s41590-020-0646-0.

Blocking elevated p38 MAPK restores efferocytosis and inflammatory resolution in the elderly

R. P. H. De Maeyer[1,*], **R. C. van de Merwe**[1,*], **R. Louie**[1], **O. Bracken**[1], **O. P. Devine**[2], **D. R. Goldstein**[3], **M. Uddin**[4,5], **A. N. Akbar**[2], **D. W. Gilroy**[1,†]

[1]Division of Medicine, University College London, London, UK

[2]Division of Infection and Immunity, University College London, London, UK

[3]Department of Internal Medicine, University of Michigan, Ann Arbor, Michigan, USA

[4]Respiratory, Inflammation and Autoimmunity, IMED Biotech Unit, AstraZeneca, Gothenburg, Sweden

[5]Respiratory Global Medicines Development, AstraZeneca, Gothenburg, Sweden

Abstract

While increasing age alters innate immune-mediated responses, the mechanisms underpinning these changes in humans are not fully understood. Using a dermal model of acute inflammation, we found that while inflammatory onset is similar between young and aged individuals, the resolution phase was significantly impaired in the elderly. There was an accumulation of immune debris compared to younger counterparts. This arose from a reduction in TIM-4, a phosphatidylserine receptor expressed on macrophages that enables engulfment of apoptotic bodies, so-called efferocytosis. Reduced TIM-4 in the elderly was caused by an elevation in macrophage p38MAPK activity. Administering an orally active p38 inhibitor to elderly individuals rescued TIM-4 expression, cleared apoptotic bodies and restored a macrophage resolution phenotype. Thus, inhibiting p38 in the elderly rejuvenated their resolution response to that of younger people. This is the first resolution defect identified in humans that has been successfully reversed, thereby highlighting the tractability of targeting pro-resolution biology to treat diseases driven by chronic inflammation.

Human life expectancy has almost doubled in the past two centuries and is continuing to rise due to advances in healthcare and improved socio-economic conditions. Ageing is a major risk factor for a plethora of chronic diseases such as atherosclerosis, Alzheimer's, COPD

† Corresponding author Professor Derek W. Gilroy, Division of Medicine, University College London, Rayne Institute, 5 University Street, London WC1E 6JF, d.gilroy@ucl.ac.uk.

*These authors contributed equally to this work

Author contributions

DWG, ANA and MU conceived the project, while DRG participated in original experimental design. RPHDM, RCvdM and DWG designed, performed and analysed all experiments, except where otherwise stated, and wrote the manuscript. RL conceived p300 experiments, and designed, performed and analysed p300 ChIP experiments. OB and RPHDM performed and analysed p300i experiments. OPD performed tissue sectioning, staining and analysis with RCvdM.

Competing interest declaration

MU is an employee of AstraZeneca and holds share in the company.

The other authors declare no competing interest.

and cancer and results in increased susceptibility to infection and a concomitant decrease in vaccine efficacy[1–3]. A unifying pathophysiology of all these disparate conditions is a dysregulated immune system. Changes in both innate and adaptive immunity with age have been well documented, though the mechanisms behind altered inflammation with age are still relatively poorly understood[4]. Ageing is associated with a state of low-grade, chronic systemic inflammation termed *inflamm-ageing*[5], but its impact on the magnitude and duration of innate immune onset and resolution is not well documented. Inflammatory onset sees the infiltration of granulocytes, particularly polymorphonuclear neutrophils (PMNs), and mononuclear myeloid cells under the control of soluble mediators and cell adhesion molecules. Resolution is also controlled in an active manner typified by the inhibition of granulocyte trafficking and dampening of pro-inflammatory signalling pathways alongside cytokine catabolism. This is followed by PMN apoptosis and subsequent timely non-phlogistic clearance by mononuclear phagocytes (monocytes and macrophages, collectively: MPs) in a process called efferocytosis[6]. This critical determinant of resolution not only eliminates debris from inflamed tissues, but also programs MPs to acquire an immune regulatory, pro-resolution phenotype conducive to terminating inflammation and promoting healing. Indeed, one suggested cause of *inflamm-ageing* is the continuous presence of cellular debris whose generation–disposal balance becomes impaired with age. This leads to a continuous and increasingly destructive cycle of immune debris accumulation resulting in perpetual activation of the inflammatory cascade[7].

We took an experimental medicines approach to understand whether inflammatory onset and/or resolution are affected by increasing age and, secondly, whether this could be reversed pharmacologically. We used a dermal model of sterile inflammation in healthy young (18–40 years) and aged (>65 years) volunteers induced by cantharidin, a topically applied vesicant that causes acantholysis and subsequent blister formation[8]. This is a robust and reproducible model that allows easy access to cells and mediators of the acute inflammatory response[9]. We found that blisters from aged participants were less exudative and erythematous within the first 24h after insult compared to those from young participants with these features becoming similar in both age groups by 72h (Fig. 1A). These differences at 24h arose from blister exudate volume and protein concentration in the elderly being almost half that of younger individuals (Fig. 1B–C). Of interest, while oedema correlated with total inflammatory cells numbers in the young cohort ($r = 0.6361$, $p < 0.0001$, $n = 35$), this correlation was lost in the elderly ($r = 0.2569$, $p = 0.1489$, $n = 33$).

In terms of blister cytokines, we found that the archetypal inflammatory mediators, TNF-α (Fig. 1E) and IL-1β (Fig. 1F) exhibited very similar profiles in young and old individuals. However, IL-6 (Fig. S1A), CCL2 (Fig. S1C), CCL7 (Fig. S1F), CXCL5 (Fig. S1I) were all lower in blisters of aged individuals at 24 h. Of these, IL-6 was the only cytokine that remained lower in old compared to young volunteers at 72 h (Fig. S1A). CXCL8 (IL-8) was also lower in blisters from the aged at 72 h, though present at the same levels in both age groups at 24 h (Fig. 1G); M-CSF was present at higher levels in blisters from aged individuals at 24 h (Fig. S1K). Total cell counts (Fig. 1H) including MPs (Fig. 1I, gating in Fig. S2) showed no age-dependent difference over time. Numbers of PMN that infiltrated at 24 h were equivalent between young and aged individuals (Fig. 1J). Importantly, and commensurate with healthy resolution, PMN numbers reduced uniformly over time in young

individuals, but did not exhibit the same temporal clearance in the older cohort (Fig. 1I). Previous reports using the cantharidin blister model examined 24 h as the peak of inflammatory onset and 72 h as a resolution time point. To characterise this further, we examined an intermediate time point in a set of young and old participants. We found no age-related or temporal changes in MP numbers (Fig. S3A), but found that PMN numbers peaked at 24 h in young volunteers and declined thereafter. In the elderly, PMN infiltrates appeared to plateau at 24 hours, with numbers not changing from 24 to 48 to 72 hours (Fig. S3B).

Next, to determine whether PMN migration is altered with age, we used IL-6, IL-8, CXCL1, CXCL5 and CCL7 at concentrations found in blister exudates from young people (1x chemokine) or from aged individuals (0.5x chemokine) in *in vitro* migration assays. Both concentrations attracted PMNs from young and old volunteers to the same extent (Fig. 1K). Moreover, PMNs from peripheral blood and those found in 24 h cantharidin blisters showed no age-related change in expression of the key chemokine receptors CXCR1 (Fig. 1L) and CXCR2 (Fig. 1M). Indeed, PMNs from young and aged donors showed no change in expression of CD16 (Fig. S3C), CD11b (Fig. S3D), CD66b (Fig. S3E) and CD62L (Fig. S3F) in either peripheral blood or cantharidin blisters. Taken together, we report that cellular infiltration and PMN phenotype was unaltered with age during the onset of inflammation. As we observed a defect in PMN clearance in the elderly indicative of failed resolution (Fig. 1J), we rationalised that this arose from changes in rates of PMN death and/or efferocytosis by blisters MPs.

During inflammatory resolution, phosphatidylserine (PS) is expressed on the surface of dead and dying cells acting as an “eat-me” signal enabling their recognition and rapid removal by MPs[6,10–12]. In this setting PS expression also acts a marker of apoptosis. Therefore, PS expression was analysed on the surface of cantharidin blister PMNs from old and young volunteers at 24 h (Fig. 2A). In contrast to younger individuals, we found that an increased proportion of the infiltrated PMNs were apoptotic (Fig. 2B–C). Commensurate with this increase in apoptotic cells in the elderly was a trend towards an accumulation of dead PMNs (Fig. 2D) and a significant increase in lactate dehydrogenase (LDH) in cell-free exudates, a marker of cell death (Fig. 2E).

To assess whether ageing affected PMN apoptosis, we isolated peripheral blood PMNs from healthy aged and young donors and cultured these cells *in vitro* to determine rates of spontaneous and stimulus-induced cell death. Viability decreased steadily at an equivalent rate in PMNs from both age groups over a 24 h period (Fig. 2F, right y-axis) concurrent with an equivalent rate of PS exposure on these same cell cultures (Fig 2F, left y-axis). In addition, stimulating PMNs from young and aged donors with TNF-α failed to show age-dependent differences in rates of PMN apoptosis (Fig. 2G). Fas stimulation was also without affect PMN apoptosis rates (Fig. S4A). TNF receptor (TNFRI/II) and Fas expression on PMNs from old and young donors was equivalent (Fig. S4B–D). Thus, while we observed impaired clearance of PMNs in the blisters of aged volunteers, these data led us to believe that the persistence of PMNs in the aged was not a consequence of their increased lifespan or failure to undergo timely apoptosis. Rather, it indicated a potential age-related defect in the efferocytosis of apoptotic bodies by MPs.

Pearson correlation analysis of the number of infiltrated MPs at 24 h versus PMN clearance ([n at 24 h] – [n at 72 h]) showed a robust correlation in young ($r = 0.5687$, $p = 0.0071$, $n = 21$, Fig. 3A). This correlation was not observed in the aged cohort ($r = 0.3418$, $p = 0.1793$, $n = 17$, Fig. 3B). Indeed, the same trend was seen from 24 h to 48 h in young, but not old people (Fig. S5A). Efferocytosis is challenging to capture *in vivo* with MPs containing apoptotic bodies, so-called Reiter cells, being rare even during active resolution. This is commensurate with efferocytosis being traditionally referred to as a highly dynamic but "silent" process, with approximately one efferocytosis event being detected in 10^5 cantharidin blister cells (0.001%, Fig. S5A). Therefore, an *ex vivo* efferocytosis assay was established to determine phagocytic capability of MPs from young and old donors (for comparison with efferocytosis *in situ*, a representative cytospin of the *ex vivo* assay is shown in Fig. S5B), in particular to identify the key stages in efferocytosis namely tethering (adherence of apoptotic cells to the surface of MPs) and engulfment. Here, MPs from 24 h cantharidin blisters were incubated with CFSE-labelled autologous apoptotic PMNs. Quantitative analysis was performed using imaging flow cytometry, (Fig. 3C). Here, in panel (i) autologous CFSE-labelled apoptotic PMNs (ACs) are shown while $CD14^+$ MPs from a human cantharidin blister (24 h) are shown in panel (ii). The images in panel (iii) depict apoptotic PMNs attached to the surface of blister MPs, so-called tethering, while panel (iv) shows MPs having engulfed apoptotic PMNs. Using this approach, we found that 60% of MPs from young donors had tethered and/or engulfed ACs, in contrast to only 20% in the elderly (AC^+ MPs, Fig. 3D). However, of these 60% in young and 20% in old, 80% of each had fully engulfed ACs (internal score > 0, Fig. 3E), thereby suggesting a defect in tethering but not in engulfment in MPs from elderly volunteers. Indeed, of the AC^+ population, fewer MPs from the elderly had tethered ACs compared to younger counterparts (Fig. 3F. The consequence of this was an overall reduction in proportions of MPs that had efferocytosed (tethered and engulfed apoptotic PMNs, Fig. 3G) in the aged. These are the cells that will undergo pro-resolution signalling, implying ageing negatively affects efferocytosis-mediated resolution. To confirm the assay could detect a change in internalisation of ACs (internal score >0), MPs were pre-treated with the actin polymerization inhibitor, cytochalasin B (Cyt B, 10 μM) for 2 h prior to efferocytosis, resulting in an inhibition of AC internalisation (Fig. S5C).

Due to the rarity and difficulty in exclusively using blister-derived MPs, we wished to establish a reliable *ex vivo* model using more abundant, yet comparable cells. We resorted to using peripheral blood MPs. We avoided using *in vitro* generated monocyte-derived macrophages (MDMs[15,16]) as they substantially differed in phenotype to cantharidin blister MPs with lower CD14 expression (Fig. S6A) and significantly upregulated expression of efferocytosis machinery (Fig. S6B–E). Freshly isolated blood MPs cultured for 24 h, however, strongly resembled 24 h cantharidin blister MPs with regard to these key markers (Fig. S6A–E). We found that the age-related efferocytosis defect was recapitulated in MPs isolated in this manner (Fig. S6F). To determine whether the observed age-dependent tethering defect (Fig. 4D–F) lay with the apoptotic cells, PMNs from old and young volunteers were allowed to apoptose, subsequently labelled with CFSE and then fed to cultured MPs. We found that apoptotic PMNs from old or young volunteers were efferocytosed equally efficiently (Fig. 3H). These data suggest that impaired efferocytosis in

the elderly does not arise from a PMN defect, which is in keeping with our observations that PMNs from both age groups apoptose at the same rate (Fig. 2 F–G) and express PS to the same extent when apoptotic (Fig. S6D). We wished to determine whether efferocytosis, as mediated by molecules such as TIM-4 and MerTK, was uniquely impaired with age compared to other forms of phagocytosis. To this end, fluorescently labelled 1 μm latex beads were used to challenge MPs from young and old donors *ex vivo*. Beads were either left in their naïve state (LB) or opsonised (OLB) to mobilise different phagocytic machinery (representative images shown in Fig. S6E). While ageing certainly resulted in the impairment of Fc-mediated and Fc-independent phagocytosis, there was a significantly more marked defect in efferocytosis *per se* (Fig. 3I). To understand the nature of age-related defective efferocytosis we investigated blister MP phenotypes. CD14, CD16 and HLA-DR all showed no differential expression with age (Fig. S7G–I). Cell surface markers typically associated with resolution including CD163 and CD206 (Fig. S7J–K) were unchanged with age while CD36 and CD51 were essentially undetectable on blister MPs in either age group (Fig. S7L–M). The integrin CD11b showed no age-dependent change either (Fig. S7N). In line with our findings regarding AC ingestion, MerTK, which is a primary mediator of AC engulfment[17,18] also showed no age-dependent alteration in expression (Fig. 4A). However, the phosphatidylserine receptor TIM-4 was significantly less expressed on MPs from aged humans (Fig. 4B). As TIM-4 is an anchoring receptor for apoptotic bodies[17,19,20], its reduced expression on MPs might explain why binding, but not engulfment of, apoptotic PMNs was impaired in aged people (Fig. 3D–E). Indeed, a TIM-4 blocking antibody was able to inhibit efferocytosis without affecting the engulfment process (Fig. 4C). Moreover, we determined that TIM-4 (Fig. S7O), but not MerTK (Fig. S7P), was downregulated on cultured MPs from aged compared to young individuals. Overall, we established that TIM-4 is a key regulator of the efferocytosis process during human inflammatory resolution and that its reduction on aged MPs resulted in impaired clearance of ACs in the elderly.

Due to its marked re-programming effects on MP function, efferocytosis is a potent pro-resolution stimulus[19,20,51] to the extent that apoptotic entities or soluble products of the efferocytosis process have been trialled in certain inflammatory conditions[21–23]. Therefore, we further probed the consequences of impaired efferocytosis on the phenotype of MPs from old and young donors. Peripheral blood monocytes were isolated from young and aged donors and cultured for 24 h before being treated with 1 ng/ml LPS and/or ACs (3:1 ratio to MPs) followed by determination of sub-cellular localisation of the p65 subunit of NFκB (pro-inflammatory) and phospho-STAT3 (pro-resolution, Fig. S8). Pro-inflammatory signalling triggered by LPS was equivalent in MPs from both age groups with ACs almost fully inhibiting LPS-mediated NFκB/p65 translocation in MPs from old and young donors (Fig. 4D). However, while ACs triggered P-STAT3 translocation within MPs from young people, they were without effect on MPs from old volunteers (Fig. 4E). Efferocytosis[24,25], and indeed STAT3 signaling in MPs[26,27], results in pro-resolution and wound healing sequelae such as TGF-β release and CCR7 upregulation. The lack of efferocytosis and subsequent pro-resolution signalling in old participants translated to the blister microenvironment where MP CCR7 expression (Fig. 4F) and TGF-β release (Fig. 4G) elevated over time in the young but failed to do so in blisters of old volunteers. In line with

what we observed *in vivo*, blocking TIM-4 resulted in a significantly impaired release of TGF-β by cultured MPs challenged with ACs (Fig. 4H).

Thus, apoptotic PMNs dampened pro-inflammatory signalling pathways in MPs from both age groups whilst triggering pro-resolution pathways in MPs from young people only. This corroborates our findings that many NFκB-regulated pro-inflammatory mediators, such as TNF-α (Fig. 1E), decline over time in both young and old blisters, whereas pro-resolution pathways such as PMN clearance and TGF-β production are seen only in the young.

As the age-related efferocytosis defect resulted from a reduction in TIM-4 on MPs, we wished to understand the molecular basis of TIM-4 expression. We found that TIM-4 expression on peripheral blood monocytes was lower in aged compared to young cohorts at both the protein level (Fig. 5A) and mRNA expression showing age-related dysfunction of Timd4 gene expression (Fig. 5B). Though very little is known regarding the regulation of TIM-4[28–32], Yang *et al.* demonstrated that its expression is regulated by p300 in murine dendritic cells. p300 is a histone acetyltransferase often located at gene promoters and enhancers and is known to participate in the expression of key molecules in inflammatory cells[29]. Therefore, we investigated whether p300 also regulates Timd4 gene expression in human monocytes and whether this pathway is affected by increased age. Chromatin immunoprecipitation on isolated blood monocytes from young and old donors, focusing on putative p300-binding sites, did lead us to identify a novel p300-binding site upstream of the *Timd4* promoter (Fig. 5C). There was equal p300 binding to the identified *Timd4* sites in MPs isolated from both young and aged donors (Fig. 5C). However, we did observe that these *Timd4* sites were less acetylated in MPs from aged donors (Fig. 5C). This suggested that while p300 binding to *Timd4* promoter sites *per se* was uninhibited, its acetyltransferase activity was impaired in aged MPs, ultimately resulting in decrease *Timd4* expression.

The activity and specificity of p300 is modulated by multiple factors including p38MAPK, a potent modulator of inflammation[33–35]. p38MAPK was of particular interest due to its involvement in age-related pathophysiology such as *inflamm-ageing* and the senescence-associated secretory phenotype (SASP[36,37]). We did not observe altered phospho-p38 levels in naïve skin MPs in old compared to young volunteers (Fig. 5E–G). However, MPs in the cantharidin skin blister did show an age-dependent increase in p-p38 levels of approximately two-fold. In comparison blister PMNs did not exhibit these changes (Fig. 5D). These findings led us to probe whether p38 could regulate TIM-4 expression in mononuclear phagocytes through p300. MPs were cultured *in vitro* in the presence of LPS to mimic a sterile inflammatory environment akin to the cantharidin blister. This inflammatory environment is sufficient to drive TIM-4 expression over time, as observed in other inflammatory contexts[28]. Inhibition of p38 using the selective inhibitor losmapimod (GW856553) significantly enhanced TIM-4 expression in MPs (Fig. 5H) concomitant with improved efferocytic function of these MPs (Fig. 5I). To examine the role of p300 in this pathway, we added p300 inhibitors in addition to p38 inhibition. We first showed that losmapimod treatment resulted in increased acetylation of the *timd4* promoter, abrogated by the addition of p300 inhibitors (Fig. 5J). The addition of p300 inhibitors also abrogated the losmapimod-mediated improvement in TIM-4 expression and efferocytosis but had no effect on a control target such as CD14 (Fig. 5K). We recapitulated these data using a separate

p300 inhibitor (A-485, Fig. S9A–C). Taken together, these data demonstrate that TIM-4 expression in humans is regulated, at least in part, by p38MAPK through the histone acetyltransferase p300. Previous, though not extensive, work on the role of p38MAPK showed it had no effect on efferocytosis[38]. However, in these experiments p38 inhibitors were added to the experimental culture system for a few hours only whereas we discovered that an incubation time of at least 48–72h is required for optimal p38 inhibition to increase TIM-4 expression and efferocytosis to be rescued.

Finally, we determined whether inhibiting p38 in elderly individuals restored MP TIM-4 levels as well as efferocytosis indices akin to that seen in young people. For this we again used losmapimod. Here, a cohort of aged volunteers were given 15 mg losmapimod, orally, twice daily for four days prior to cantharidin (Fig. 6A). Drug compliance was assessed by analysing LPS-stimulated whole blood TNF-α (Fig. S10A) and IL-6 (Fig. S10B) release. Interestingly, we noted that losmapimod treatment reduced baseline serum TNF-α (Fig. 6B) and IL-6 levels (Fig. S10C), highlighting the effect of inhibiting constitutively elevated p38 in the elderly on "*inflamm-ageing*"[39]. However, losmapimod did not inhibit cantharidin-induced blister TNF-α levels (Fig. 6C), IL-6 levels (Fig. S10D), or PMN infiltration (Fig. 6D) but did result in less exudative blisters compared to controls and blisters from young donors (Fig. S10E–F). Losmapimod did restore total protein levels to those seen in young by 72 hours (Fig. S10G). This implies that while losmapimod inhibits the systemic symptoms of *inflamm-ageing* it does not affect the acute onset response to tissue damage in skin.

However, in terms of resolution, we found that losmapimod treatment resulted in a significant reduction in the accumulation of $CD16^{hi}$/Annexin V^{+} early apoptotic PMNs in blisters of old volunteers (Fig. 6E). Indeed, this impaired clearance of apoptotic cell debris in the elderly mirrored an increase in extracellular LDH levels, which as with numbers of ACs was reversed with losmapimod (Fig. 6F). These data suggest that inhibition of p38 reverses the accumulation of apoptotic PMNs and immune debris at inflammatory sites in the elderly. These restorative effects of losmapimod on resolution were associated with increased TIM-4 expression on blister MPs (Fig. 6G) but was without effect on MerTK (Fig. 6H), mimicking our *in vitro* observations (Fig. 5H). Importantly, improvement in TIM-4 expression on MPs from the aged led to a restoration of the correlation between MP numbers and PMN clearance in cantharidin blisters (Fig. 6I). In a separate cohort to that shown in Fig. 3A–B, we again demonstrated that young people exhibited a strong correlation between MP infiltration and PMN clearance that was lost in healthy elderly people (Fig. 6I). Losmapimod treatment completely restores this correlation and key pro-resolution index in the aged (Fig. 6I). This once again highlights the resolution-restorative effects of p38 inhibition in aged humans through a TIM-4-dependent mechanism that corrected age-related efferocytosis defects. CCR7 expression on blisters MPs (Fig. 6J) and blister TGF-β levels (Fig. 6K) were restored in the losmapimod treated cohort compared to untreated, highlighting the restoration of efferocytosis-dependent sequelae in blister samples from losmapimod treated elderly participants.

In this study, we found that aged humans experience the same rate of granulocyte infiltration and synthesis of some, but not all pro-inflammatory cytokines as do younger individuals during acute sterile inflammation. However, we discovered that the other end of the

inflammatory spectrum, resolution, was impaired in the elderly due to MP dysfunction. The nature of this dysfunction was a reduced capacity for efferocytosis due to decreased TIM-4 expression. We revealed that this reduction was brought about by an age-related increase in p38 activity in MPs, which in turn resulted in the histone acetyltransferase p300 not activating the *tim4* promoter. Pharmacological blockade of p38 both *in vitro* and *in vivo* in humans resulted in a reversal of the efferocytosis defect and the restoration of proper inflammatory resolution.

We posit that resolution pathways are critical in foregoing chronic inflammation such as that observed in the form of *inflamm-ageing*[40,41]. Specifically, we describe a failure of the immune system to shut down acute inflammation due to a lack of efferocytosis, imparting on MPs a persistent pro-inflammatory phenotype. This, combined with the resultant build-up of cellular debris drives *inflamm-ageing*. It has been established that efferocytosis is a key step for switching off inflammation and bringing about a return to homeostasis through the upregulation of wound healing pathways[42–44] or forming an optimal stage for the formation of adaptive immune responses[45,46]. A build-up of cellular debris has been suggested as a pathogenic factor in certain autoimmune conditions[47–49] and has been suggested to be involved in age-related pathology[7]. Our findings in young versus old humans are in support of this idea and demonstrate the molecular mechanisms underlying the pathogenesis of "*inflamm-aging*" in humans and show that this process can be reversed pharmacologically.

Multiple studies have attempted to address whether ageing affects PMN migration, function and longevity[50,51]. While some have shown that PMN migration is impaired with increased age, these findings were made in murine models of peritonitis[52]. In contrast, our work and the work of others using Senn's human experimental skin window model, which is a skin abrasion model isolated with a sterile chamber filled with autologous serum, have clearly demonstrated no age-related difference in PMN migration rates using skin and suggest that these disparities are likely a species related phenomenon[53,54]. In terms of cell death, the precise role of p38 MAPK in PMN apoptosis is controversial[55–57]. Certainly, we found that both spontaneous or stimulated PMN apoptosis occurs at the same rate in young and old humans.

This, alongside equivalent levels of p-p38MAPK in PMN from young and elderly volunteers, suggests that rates of PMN death is independent of age at least in humans. Of note, it was on only mononuclear phagocytes from old volunteers that had higher p-p38 expression levels. It is therefore unlikely that apoptosis *per se* underlies the pathophysiology of *garb-ageing* and by extension, *inflamm-ageing*. Of note however, was a highly positive correlation between TNF-α levels and PMN numbers in the blisters of young people (Fig. S5B), which was lacking in our elderly cohort (Fig. S5C). The role of TNF-α in PMN trafficking is complex with TNF-α having an indirect effect on the accumulation of PMNs at site of inflammation via the upregulation of potent neutrophilic chemoattractants, notably IL-8 and LTB_4[58] and the stimulation of vascular endothelial cells to facilitate PMNs transport[59]. Despite this discordance in elderly volunteers, the numbers of infiltrating PMNs were consistent in the blisters of both age groups. This indicates that the indirect role TNF-α plays in orchestrating PMN trafficking in young people is lost with increasing age and is perhaps superseded by an alternative mechanism beyond TNF-α as we get older[2,8,9]. This

becomes important in the consideration of developing novel therapeutic strategies to target PMN-driven pathologies in the aged.

Experiments examining the impact of age on resolution and efferocytosis have been carried out by others, including Arnardottir and colleagues[52], who showed an age-dependent reduction in efferocytosis in rodent bone marrow-derived macrophages and impaired resolution during peritonitis. Frisch *et al.* published similar findings where fluorescently-labelled apoptotic PMNs were injected into mice and their clearance by bone marrow macrophages was found to be impaired in old compared to young mice[60]. These authors found that various elements of the efferocytosis machinery, namely TAM receptors (Tyro3, MerTK and Axl) and bridging molecules, were downregulated on macrophages in aged mice thereby providing a potential explanation for their findings. However, we examined Axl in only a very small cohort of individuals but saw no trends towards a difference (data not shown) and we found no age-dependent difference in blood or blister monocyte/macrophage MerTK expression (Fig. 4A, S7). Frisch and colleagues did not comment on whether TIM-4 expression differed between young and old rodents. Indeed, we found that while TIM-4 is expressed on human monocytes and skin/inflammatory MPs we did not see TIM-4 expression on circulating mouse monocytes (data not shown). It is present, however, on tissue-resident MPs[61–63]. Moreover, unlike in humans, TIM-4 expression in mouse tissue MPs showed no age-dependent decrease (data not shown). The reason for this is unclear, but possibly occurs due to a lack of lifelong exposure to antigen and other injurious stimuli that drive inflammatory cascades that condition or educate the innate immune system. Therefore, published studies showing age-related decreases in inflammatory onset in mice[52] may not be translatable in aged humans.

In terms of translation, our finding suggests that inhibition of p38 could accelerate wound healing in the elderly. Persistent inflammation is characterized by over-activated macrophages, exuberant release of pro-inflammatory cytokines and a decrement in wound healing factors, events congruent with failed resolution. Therefore, from our work, we propose that this prolonged inflammation phase in the elderly arises from impaired pro-resolution processes, namely efferocytosis, and that local application of a p38 inhibitor could represent a novel treatment for age-related wound healing defects.

In addition, our findings highlight a potential usage for p38 blockade to optimise vaccine efficacy in the elderly. We found previously that pro-resolution processes enhance adaptive immunity to the inciting antigen[45,46]. By corollary, dysregulating pro-resolution pathways resulted in sub-optimal immune memory. As we established that resolution is defective in the elderly, and as vaccine efficacy declines with age, we propose that perhaps restoring pro-resolution processes using p38 inhibitors at the time of vaccination could rejuvenate immune responses to antigens in the aged. Indeed, a recent paper has shown that antigen-specific immunity in the skin of elderly volunteers can be enhanced following inhibition of p38[64]. Ultimately, we believe the approach of blocking p38 in older humans has potential applications in vaccination, a process commonly associated with worse outcomes with increased age[3].

In summary, while its well appreciated that aspects of innate and adaptive immunity are defective in the elderly, the impact of age acute inflammatory cascades in humans is less well described. Here, we have shown for the first time that the nature and progression of the onset phase of acute inflammation is ostensibly equivalent in old versus young individuals. However, resolution of the response is defective in the elderly. Specifically, we found that MPs lost their ability to clear dead cells in a process that is indispensable in preventing the development of chronic inflammation and wound healing complications. This so-called efferocytosis is largely regarded as one of the single most important determinants for inflammatory resolution. Moreover, in addition to identifying a *bono fide* resolution defect in humans we succeeded in its reversal by using short-term p38 inhibition. This is the first resolution defect that has been successfully reversed thereby highlighting the tractability of targeting pro-resolution biology to treat diseases driven by non-resolving inflammation.

Methods

Ethics Statement

These studies were approved by the UCL Research Ethics Committee (Ref: 5061/001) and the National Research Ethics Service. Written informed consent was obtained from all volunteers.

Subject recruitment

Healthy, non-smoking adult males and females aged 18 and over (≥65 years was considered aged) were recruited. A representative cohort of study volunteers was based on the following exclusion criteria:

- Regular use or use up to 1 month prior to participation in the study, of medications classed as anti-inflammatories, immunomodulatory drugs or antibiotics. This applied to over-the-counter and prescription-only drugs.
- Cancer, kidney disease, liver disease, lung disease, muscle disease, autoimmune disease, inflammatory/immune disease, neurological disease, chronic infection, skin disorders and blood disorders.
- A history of heart attack, stroke, coronary artery bypass, cancer, infections that required hospitalisation, organ transplant, surgery by general anaesthetic, major trauma or major burns, within the 2 years prior to participation in the study.

Liver and cardiac function tests were performed on subjects stratified to the losmapimod group. All subjects were asked to avoid heavy alcohol consumption and intense exercise during the study. A summary of the cohort is given in table 2.1.

Cantharidin blisters

Cantharidin blisters were raised and processed as previously described[9,65,66]. Briefly, blisters were elicited by applying 12.5 μl of 0.1% w/v cantharidin (Cantharone, Dormer Laboratories, Canada) to two sites on the ventral aspect of the forearm. One blister was aspirated on day 1 (24 hours) following induction, the other on day 3 (72 hours). For *ex vivo* efferocytosis experiments, both blisters were aspirated at 24 hours and pooled before

enumeration of cells. For this purpose, mononuclear cells were enumerated by using Turk's solution and examining nuclear and cytoplasmic morphology.

Punch biopsies and immunofluorescence

Punch biopsies of normal skin were taken from the medial, proximal, volar aspect of the forearm and snap frozen in OCT compound (Sakura TissueTek) using liquid nitrogen. 6μm cryosections were acquired on poly-L-lysine coated glass slides. Sections were fixed in acetone and ethanol prior to storage at −80°C.

Thawed sections were labelled overnight using anti-pp38 (polyclonal, Abcam ab38238, 1:80) and anti-CD163 (clone RM3/1, Abcam ab17051, 1:100) antibodies. Secondary staining was performed using AlexFluor488 (Life Technologies A11008) and AlexaFluor647 (Life Technologies A21240) labelled antibodies respectively. Slides were mounted using VECTASHIELD Antifade Mounting Medium with 4′,6-diamidino-2-phenylindole (DAPI) (Vector Labs, H-1000).

Images were acquired on the AxioScan Z1 slide scanner using Zen Blue V2.3 (ZEISS) and quantified by two independent analysts using ImageJ V2.0.0-rc-69/1 with CellCounter plugin.

Losmapimod administration

Subjects stratified to the losmapimod group received oral losmapimod (GW856553) twice daily for 4 days (provided by GlaxoSmithKline under a Medical Research Council Industrial Collaboration Agreement). The dose of 15 mg of losmapimod twice daily used in this study was chosen based on the safety profiles, pharmacokinetics and pharmacodynamics of losmapimod observed in GlaxoSmithKline phase I and II studies[66]. On day 4 of losmapimod administration cantharidin blisters were elicited.

To assess compliance, ex vivo whole-blood LPS stimulation assays were performed before and 4 days after losmapimod treatment[68]. Briefly, peripheral blood was cultured with LPS (0–1 mg/mL) for 24 hours (37°C in a 5% CO2 atmosphere). Levels of TNF-α and IL-6 in plasma were assessed by Cytometric Bead Array (CBA; BD Biosciences).

Monocyte isolation

Human peripheral blood monocytes were isolated using the RosetteSep monocyte isolation kit (Stemcell Technologies). Whole blood was incubated with 12.5 μl antibody cocktail per ml of blood for 20 minutes before being diluted 1:1 with HBSS (Mg^{2+}/Ca^{2+} free, Invitrogen). This was layered onto Ficoll Paque PLUS (GE Healthcare) and centrifuged for 15 minutes at 1,000x *g* with minimal acceleration and braking. Monocyte layers were isolated and washed three times at low speeds. Finally, monocytes were enumerated by haemocytometer and trypan blue exclusion before analysis or plating on 24-well UpCell plates (Thermofisher) at 5×10^5 cells/well in X-Vivo 15 media (Gibco) containing 10% pooled human (AB) serum (Sigma Aldrich), 2 mM L-gln (Gibco) and 1x penicillin/streptomycin (Gibco). MPs used in functional assays were cultured for 24 h prior to use. Monocyte purity and viability post-isolation was found to be >90%.

Neutrophil isolation

Human blood neutrophils were isolated using dextran sedimentation. Briefly, 10% dextran (M_r: 200,000 – 300,000, MP Biomedicals) was added to 20 ml of blood and left to sediment for one hour. The leukocyte rich plasma was layered onto Ficoll Paque PLUS (GE Healthcare) and centrifuged for 15 minutes at 1,000x *g* with minimal acceleration and braking. The mononuclear cell layer and plasma were discarded, and residual erythrocytes removed from the pelleted neutrophils using ACK lysis. Pellets were washed once before being resuspended in RPMI 1640 supplemented with 0.1% BSA. Freshly isolated PMNs were >95% pure and viable as confirmed by trypan blue exclusion. Cells were incubated at 37°C for 16–24 hours, enumerated by haemocytometer and examined for apoptosis using annexin V/7-AAD staining (BD biosciences) and flow cytometry. Neutrophils tended to be >75% apoptotic using this method, with only maximally 5% showing necrotic characteristics.

Flow cytometry

A maximum of 5×10^5 cells were stained using a combination of antibodies (Table 2.2). All staining was performed in PBS + 10% FCS, except where multiple Brilliant Violet dyes were used in the same panel. Here, cells were stained in Brilliant Stain Buffer (BD Biosciences). All staining was done in the presence of 5 μl Fc receptor blocking antibody (Biolegend) per sample. Stains were performed for 30 minutes at 4 ^{o}C and followed by two washes with PBS containing 2% FCS and 2 mM EDTA before fixation in 0.5% PFA in PBS.

For phosflow cytometry, cells were surface stained and fixed with cytofix buffer (BD Biosciences). This was followed by permeabilisation with ice-cold Perm Buffer III (BD Biosciences) and staining with antibodies for phospho-p38.

Apoptotic cells were detected using the Annexin V staining kit (BD biosciences) according to manufacturer's protocol.

Samples were acquired on an LSR Fortessa (BD Biosciences). Analysis was performed using FlowJo (Treestar Inc.).

Phagocytosis Assays

Apoptotic neutrophils (16–24 h post isolation) were stained with 2 μM CFDA-SE (Life technologies) as per the manufacturer's protocol. Stained ACs were enumerated and added to mononuclear phagocyte (MP) populations at a ratio of 5 ACs to 1 monocyte in the cantharidin blister or 3:1 with blood-derived MPs. Green fluorescent latex beads (Sigma Aldrich), where applicable opsonised using plasma from healthy young donors for 1 h, were given to MPs at 10 beads to 1 MP. Challenged MPs were co-cultured at 37 ^{o}C for 30 minutes and then immediately placed on ice. Cells were harvested and culture wells washed once with PBS containing 4 mg/ml lidocaine and 10 mM EDTA. All samples were stained with CD14-AF647 with/without DAPI (Sigma Aldrich, 1 μg/ml) in PBS containing 10% FCS and 5% Fc receptor blocking antibody for 30 minutes at 4 ^{o}C. Cells were washed and resuspended in 25 μl PBS containing 4% PFA before acquisition on an ImageStreamX Mk2 (Amnis). ImageStream files were analysed using IDEAS software (Amnis). First, total cells

were gated using area of the CD14 signal and the aspect ratio of the CD14 signal. Single cells are then gated on CD14 expression (Intensity) and DAPI to identify $CD14^+$ mononuclear phagocytes. MPs were subsequently plotted on a histogram against CFSE. MPs not exposed to labelled ACs were used as an FMO control. AC^+ MPs consisted of a population of MPs that had either bound to and/or ingested ACs. To distinguish MPs that had ingested AC versus those that had merely bound ACs, an internalization score was used. A mask that erodes the signal by 7 pixels was created for the CD14 channel to exclude CFSE found on the membrane of MPs. The IDEAS internalization score was then used to differentiate internal (Score > 0) vs external (Score < 0) CFSE signal. For cantharidin blister efferocytosis experiments, a minimum of 100 $CD14^+$ events and for *in vitro* experiments, a minimum of 5000 $CD14^+$ events was acquired. Actin polymerisation was inhibited using 2-hour pre-treatment of MPs with 10 μM cytochalasin B (Sigma). For blocking experiments, cells were pre-treated for 30 min with 5 μg/ml anti-TIM-4 (clone 9F4, 354002 Biolegend, or polyclonal, AF2929 R&D Systems). For confirmation of phagocytosis by microscopy, blister cells or cultured MPs were cytospun and stained using the Shandon Kwik-Diff kit (Thermo Fisher) according to manufacturer's instructions.

Nuclear localisation of Transcription Factors

MPs were stimulated for 30 minutes with 1 ng/ml LPS and/or 3:1 ACs:MPs before being immediately fixed in 4% PFA in PBS for 15 minutes at room temperature. Cells were stained using CD14-AF647 as above. After washing, cells were permeabilised using 0.1% Igepal CA-630 (Sigma Aldrich) in PBS containing 10% FCS for 20 minutes before addition of 1μg/ml DAPI, 5% anti-NFκB(p65)-PE and 5% anti-P-STAT-3-AF488 for a further 30 min. Cells were washed twice in PBS containing 0.1% Igepal CA-630, 2% FCS and 2 mM EDTA before finally being resuspended in 25 μl PBS containing 2 mM EDTA. Samples were acquired on the ImageStreamX Mk2 (Amnis). A minimum of 5000 $CD14^+$ events was recorded. Signal overlap was determined by the IDEAS (Amnis) bright detail similarity score. This was done to compare overlap between DAPI and NFκB, as well as DAPI and P-STAT3.

qRT-PCR

Total RNA from was extracted with TRIzol Reagent (Invitrogen). Sample concentration and purity was determined using a NanoDrop™ 1000 Spectrophotometer and cDNA was synthesised using the qScript cDNA Synthesis Kit (Quanta). Specific genes were amplified and quantified by quantitative Real Time-PCR, using the PerfeCTa SYBR Green FastMix (Quanta) on an MX3000p system (Agilent). Primer sequences are shown in Table 2.3. The relative amount of mRNA was calculated using the comparative Ct method and normalised to the expression of cyclophilin[69].

ChIP

ChIP experiments were performed and analysed as described[68] except cells were cross-linked with 2mM of disuccinimidyl glutarate (Thermo Scientific) for 20 min, followed by 10 min with 1% formaldehyde solution (Thermo Scientific). The antibodies employed include p300 (#PA1–848, ThermoFisher, 5μg) and H3K27ac (ab4729, Abcam, 3μg). Oligonucleotides used are shown in Table 2.3. To control for non-specific binding, a 78 base

pair fragment in a gene desert on human chromosome 12 using commercial oligonucleotides (#71001, ActiveMotif) were used.

Transwell migration assays

Isolated neutrophils were resuspended at 1.5×10^6 cells/ml incomplete RPMI medium. 200 µl (3×10^5 cells) was transferred to a 24-well transwell insert (6.5 mm diameter, 5 µm pore size, polycarbonate, Corning) in wells containing 600 µl of complete RPMI with or without chemokines. Medium alone served as the negative control. 16 ng/ml IL-16 and CCL7, and 8 ng/ml CXCL1, CXCL5 and CXCL8 were used as "1x chemokine" (all from Peprotech). 0.5x used half these concentrations. PMNs were left to migrate at 37 ^oC, 5% CO_2 for 15 minutes. Remaining medium and cells was removed from the transwell inserts and any cells adhered to the well side of the membrane were harvested using cell dissociation media (Gibco). Unadhered and adhered migrated cells were enumerated using a CyQUANT (ThermoFisher Scientific) DNA staining kit according to manufacturer's instructions. A standard curve of DNA concentrations was run in duplicate.

Cytokine and solute measurements

Cell-free cantharidin blister exudates and monocyte culture supernatants were assayed for total protein content using a Bradford assay (Bio-Rad) as per the manufacturer's instructions.

TGF-β levels were determined using a single-plex sandwich ELISA (Affymetrix eBioscience). The assay was performed according to the manufacturer's instructions.

Other cytokines were measured using an RnD Luminex Screening Assay (Bio-Techne) or cytometric bead array (BD Biosciences). Samples were run in duplicate and the assays were performed according to the manufacturer's instructions.

Lactate dehydrogenase (LDH) activity was measured in cell-free cantharidin blister exudates using an LDH cytotoxicity kit (Thermo Scientific) according to manufacturer's instructions.

Calculations and Statistical Analysis

Statistical analysis of these data was performed using GraphPad Prism version 7.01/8.3 (GraphPad Software, San Diego, California, USA). Every set of data was subjected to normality and lognormality testing on GraphPad Prism. Where data were found to be part of a lognormal distribution, they are shown on a log scale with geometric means and geometric standard deviation (s.d.) where applicable. Normal data are shown as arithmetic means with s.d. where applicable. Parametric tests were carried out on log transformed values for lognormal, and on untransformed values for normal data. Data that did not pass normality tests were analysed using non-parametric statistical tests. Temporal, intra-age group differences were assessed using paired tests. Correlations were computed using the Pearson coefficient method. Differences were considered significant when $P<0.05$ (*), $P<0.01$ (**), $P<0.001$(***) and $P<0.0001$ (****).

Supplementary Material

Refer to Web version on PubMed Central for supplementary material.

Acknowledgements

We would like to thank all the volunteers who participated in this study, Ms Michelle Berkeley and Ms Megan Harries for assistance with recruitment, Dr Veronique Birault and Dr Iain Laws, Dr Ruchira Glaser, Dr Lea Sarov-Blat, and Dr Robert Henderson from GlaxoSmithKline for provision of losmapimod (MICA agreement with the MRC), specifically the losmapimod team at GSK for organising the dispatch of the clinical supply of the drug in this investigator-led study. We extend our gratitude to our colleagues for invaluable discussion, especially Dr Emma Chambers.

RPH De Maeyer was supported by an AstraZeneca-MRC Industrial CASE PhD Studentship (MR/J006610/1) jointly awarded to the supervisors DW Gilroy (UCL) and M Uddin (AZ). RC van de Merwe was funded by the MRC Grand Challenge in Experimental Medicine (MICA) grant (MR/M003833/1) awarded to AN Akbar and DW Gilroy. DW Gilroy was further funded by the Wellcome Trust.

References

1. Partridge L, Deelen J & Slagboom EP Facing up to the global challenges of ageing. Nature 561, 45–56 (2018). [PubMed: 30185958]
2. Thompson WW et al. Mortality Associated With Influenza and Respiratory Syncytial Virus in the United States. Jama 289, 179–186 (2003). [PubMed: 12517228]
3. Goodwin K, Viboud C & Simonsen L Antibody response to influenza vaccination in the elderly: A quantitative review. Vaccine 24, 1159–1169 (2006). [PubMed: 16213065]
4. Shaw AC, Goldstein DR & Montgomery RR Age-dependent dysregulation of innate immunity. Nature reviews. Immunology 13, 875–87 (2013).
5. Franceschi C et al. Inflamm-aging. An evolutionary perspective on immunosenescence. Annals of the New York Academy of Sciences 908, 244–54 (2000). [PubMed: 10911963]
6. Savill J et al. Macrophage phagocytosis of aging neutrophils in inflammation. Programmed cell death in the neutrophil leads to its recognition by macrophages. Journal of Clinical Investigation 83, 865–875 (1989).
7. Franceschi C, Garagnani P, Vitale G, Capri M & Salvioli S Inflammaging and 'Garb-aging'. Trends in endocrinology and metabolism: TEM 28, 199–212 (2017). [PubMed: 27789101]
8. Piérard-Franchimont C & Piérard G Cantharidin-induced acantholysis. The American Journal of dermatopathology 10, 419–23 (1988). [PubMed: 3228189]
9. Jenner W et al. Characterisation of leukocytes in a human skin blister model of acute inflammation and resolution. PloS one 9, e89375 (2014). [PubMed: 24603711]
10. Ariel A & Ravichandran KS 'This way please': Apoptotic cells regulate phagocyte migration before and after engulfment. European journal of immunology 46, 1583–6 (2016). [PubMed: 27345468]
11. Fond AM & Ravichandran KS Clearance of Dying Cells by Phagocytes: Mechanisms and Implications for Disease Pathogenesis. Advances in experimental medicine and biology 930, 25–49 (2016). [PubMed: 27558816]
12. Segawa K & Nagata S An Apoptotic 'Eat Me' Signal: Phosphatidylserine Exposure. Trends Cell Biol 25, 639–650 (2015). [PubMed: 26437594]
13. Bannenberg GL et al. Molecular Circuits of Resolution: Formation and Actions of Resolvins and Protectins. J Immunol 174, 4345–4355 (2005). [PubMed: 15778399]
14. Navarro-Xavier RA et al. A new strategy for the identification of novel molecules with targeted proresolution of inflammation properties. Journal of immunology (Baltimore, Md.: 1950) 184, 1516–25 (2010).
15. Sica A & Mantovani A Macrophage plasticity and polarization: in vivo veritas. The Journal of clinical investigation 122, 787–95 (2012). [PubMed: 22378047]
16. Gordon S Alternative activation of macrophages. Nature Reviews Immunology 3, 23–35 (2003).

17. Nishi C, Toda S, Segawa K & Nagata S Tim4- and MerTK-mediated engulfment of apoptotic cells by mouse resident peritoneal macrophages. Molecular and cellular biology 34, 1512–20 (2014). [PubMed: 24515440]
18. Tibrewal N et al. Autophosphorylation Docking Site Tyr-867 in Mer Receptor Tyrosine Kinase Allows for Dissociation of Multiple Signaling Pathways for Phagocytosis of Apoptotic Cells and Down-modulation of Lipopolysaccharide-inducible NF-κB Transcriptional Activation. J Biol Chem 283, 3618–3627 (2008). [PubMed: 18039660]
19. Miyanishi M et al. Identification of Tim4 as a phosphatidylserine receptor. Nature 450, 435–9 (2007). [PubMed: 17960135]
20. Park D, Hochreiter-Hufford A & Ravichandran KS The phosphatidylserine receptor TIM-4 does not mediate direct signaling. Current biology: CB 19, 346–51 (2009). [PubMed: 19217291]
21. Bonnefoy F et al. Apoptotic cell infusion treats ongoing collagen-induced arthritis, even in the presence of methotrexate, and is synergic with anti-TNF therapy. Arthritis Res Ther 18, 184 (2016). [PubMed: 27516061]
22. Ren Y et al. Apoptotic Cells Protect Mice against Lipopolysaccharide-Induced Shock. J Immunol 180, 4978–4985 (2008). [PubMed: 18354223]
23. Kojima Y et al. CD47-blocking antibodies restore phagocytosis and prevent atherosclerosis. Nature 536, 86–90 (2016). [PubMed: 27437576]
24. Fadok V et al. Macrophages that have ingested apoptotic cells in vitro inhibit proinflammatory cytokine production through autocrine/paracrine mechanisms involving TGF-beta, PGE2, and PAF. Journal of Clinical Investigation 101, 890–8 (1998).
25. Huynh M-LN, Fadok VA & Henson PM Phosphatidylserine-dependent ingestion of apoptotic cells promotes TGF-beta1 secretion and the resolution of inflammation. The Journal of clinical investigation 109, 41–50 (2002). [PubMed: 11781349]
26. Yi Z et al. A novel role for c-Src and STAT3 in apoptotic cell-mediated MerTK-dependent immunoregulation of dendritic cells. Blood 114, 3191–8 (2009). [PubMed: 19667404]
27. Soki FN et al. Polarization of prostate cancer-associated macrophages is induced by milk fat globule-EGF factor 8 (MFG-E8)-mediated efferocytosis. The Journal of biological chemistry 289, 24560–72 (2014). [PubMed: 25006249]
28. Hilligan KL, Connor LM, Schmidt AJ & Ronchese F Activation-Induced TIM-4 Expression Identifies Differential Responsiveness of Intestinal CD103+ CD11b+ Dendritic Cells to a Mucosal Adjuvant. Plos One 11, e0158775 (2016). [PubMed: 27379516]
29. Yang B et al. Histone acetyltransferease p300 modulates TIM4 expression in dendritic cells. Scientific Reports 6, 21336 (2016). [PubMed: 26899911]
30. Yang P-CC et al. TIM-4 expressed by mucosal dendritic cells plays a critical role in food antigen-specific Th2 differentiation and intestinal allergy. Gastroenterology 133, 1522–33 (2007). [PubMed: 17915221]
31. Rodriguez-Manzanet R et al. TIM-4 expressed on APCs induces T cell expansion and survival. Journal of immunology (Baltimore, Md.: 1950) 180, 4706–13 (2008).
32. Feng B-S et al. Disruption of T-cell immunoglobulin and mucin domain molecule (TIM)–1/TIM4 interaction as a therapeutic strategy in a dendritic cell–induced peanut allergy model. J Allergy Clin Immun 122, 55–61.e7 (2008). [PubMed: 18547633]
33. Wang Q-E et al. p38 MAPK- and Akt-mediated p300 phosphorylation regulates its degradation to facilitate nucleotide excision repair. Nucleic Acids Res 41, 1722–1733 (2013). [PubMed: 23275565]
34. Saha RN, Jana M & Pahan K MAPK p38 Regulates Transcriptional Activity of NF-κB in Primary Human Astrocytes via Acetylation of p65. J Immunol 179, 7101–7109 (2007). [PubMed: 17982102]
35. Poizat C, Puri P, Bai Y & Kedes L Phosphorylation-Dependent Degradation of p300 by Doxorubicin-Activated p38 Mitogen-Activated Protein Kinase in Cardiac Cells. Mol Cell Biol 25, 2673–2687 (2005). [PubMed: 15767673]
36. Tchkonia T, Zhu Y, van Deursen J, Campisi J & Kirkland JL Cellular senescence and the senescent secretory phenotype: therapeutic opportunities. The Journal of clinical investigation 123, 966–72 (2013). [PubMed: 23454759]

37. Campisi J Aging, Cellular Senescence, and Cancer. Annu Rev Physiol 75, 685–705 (2013). [PubMed: 23140366]
38. Bewley MA et al. Differential Effects of p38, MAPK, PI3K or Rho Kinase Inhibitors on Bacterial Phagocytosis and Efferocytosis by Macrophages in COPD. PLOS ONE 11, e0163139 (2016). [PubMed: 27680884]
39. Pedersen M et al. Circulating levels of TNF-alpha and IL-6-relation to truncal fat mass and muscle mass in healthy elderly individuals and in patients with type-2 diabetes. Mechanisms of Ageing and Development 124, 495–502 (2003). [PubMed: 12714258]
40. Fullerton JN & Gilroy DW Resolution of inflammation: a new therapeutic frontier. Nature reviews. Drug discovery 15, 551–67 (2016). [PubMed: 27020098]
41. Gilroy D & Maeyer R New insights into the resolution of inflammation. Seminars in immunology 27, 161–8 (2015). [PubMed: 26037968]
42. Laplante P et al. MFG-E8 Reprogramming of Macrophages Promotes Wound Healing by Increased bFGF Production and Fibroblast Functions. The Journal of investigative dermatology 137, 2005–2013 (2017). [PubMed: 28526301]
43. Hesketh M, Sahin KB, West ZE & Murray RZ Macrophage Phenotypes Regulate Scar Formation and Chronic Wound Healing. International journal of molecular sciences 18, (2017).
44. Khanna S et al. Macrophage dysfunction impairs resolution of inflammation in the wounds of diabetic mice. PloS one 5, e9539 (2010). [PubMed: 20209061]
45. Newson J et al. Inflammatory Resolution Triggers a Prolonged Phase of Immune Suppression through COX-1/mPGES-1-Derived Prostaglandin E2. Cell Reports 20, 3162–3175 (2017). [PubMed: 28954232]
46. Newson J et al. Resolution of acute inflammation bridges the gap between innate and adaptive immunity. Blood 124, 1748–64 (2014). [PubMed: 25006125]
47. Gaipl U et al. Clearance of apoptotic cells in human SLE. Current directions in autoimmunity 9, 173–87 (2006). [PubMed: 16394661]
48. Green D, Oguin T & Martinez J The clearance of dying cells: table for two. Cell death and differentiation 23, 915–26 (2016). [PubMed: 26990661]
49. Nagata S, Hanayama R & Kawane K Autoimmunity and the clearance of dead cells. Cell 140, 619–30 (2010). [PubMed: 20211132]
50. Fulop T et al. Signal transduction and functional changes in neutrophils with aging. Aging Cell 3, 217–226 (2004). [PubMed: 15268755]
51. Tortorella C et al. Spontaneous and Fas-induced apoptotic cell death in aged neutrophils. Journal of clinical immunology 18, 321–9 (1998). [PubMed: 9793824]
52. Arnardottir HH, Dalli J, Colas RA, Shinohara M & Serhan CN Aging delays resolution of acute inflammation in mice: reprogramming the host response with novel nano-proresolving medicines. Journal of immunology (Baltimore, Md.: 1950) 193, 4235–44 (2014).
53. Biasi D et al. Neutrophil migration, oxidative metabolism, and adhesion in elderly and young subjects. Inflammation 20, 673–81 (1996). [PubMed: 8979154]
54. Senn H, Holland J & Banerjee T Kinetic and comparative studies on localized leukocyte mobilization in normal man. J Laboratory Clin Medicine 74, 742–56 (1969).
55. Larbi A et al. The role of the MAPK pathway alterations in GM-CSF modulated human neutrophil apoptosis with aging. Immunity & ageing : I & A 2, 6 (2005). [PubMed: 15743527]
56. Sheth K, Friel J, Nolan B & Bankey P Inhibition of p38 mitogen activated protein kinase increases lipopolysaccharide induced inhibition of apoptosis in neutrophils by activating extracellular signal-regulated kinase. Surgery 130, 242–248 (2001). [PubMed: 11490356]
57. Frasch CS et al. p38 Mitogen-activated Protein Kinase-dependent and -independent Intracellular Signal Transduction Pathways Leading to Apoptosis in Human Neutrophils. J Biol Chem 273, 8389–8397 (1998). [PubMed: 9525949]
58. Smart S & Casale T TNF-alpha-induced transendothelial neutrophil migration is IL-8 dependent. Am J Physiology 266, L238–45 (1994).

59. Moser R, Schleiffenbaum B, Groscurth P & Fehr J Interleukin 1 and tumor necrosis factor stimulate human vascular endothelial cells to promote transendothelial neutrophil passage. J Clin Invest 83, 444–455 (1989). [PubMed: 2643630]

60. Frisch B, Hoffman C, Latchney S, LaMere M, Myers J, Ashton J, Li A, Saunders J, Palis J, Perkins A, McCabe A, Smith J, McGrath K, Rivera-Escalera F, McDavid A, Liesveld J, Korshunov V, Elliott M, MacNamara K, Becker M, Calvi L Aged marrow macrophages expand platelet-biased hematopoietic stem cells via Interleukin1B JCI Insight 5(10) (2019).

61. Foks AC et al. Blockade of Tim-1 and Tim-4 Enhances Atherosclerosis in Low-Density Lipoprotein Receptor-Deficient Mice. Arteriosclerosis, thrombosis, and vascular biology 36, 456–65 (2016).

62. Albacker L et al. TIM-4, expressed by medullary macrophages, regulates respiratory tolerance by mediating phagocytosis of antigen-specific T cells. Mucosal immunology 6, 580–90 (2013). [PubMed: 23149665]

63. Wong K et al. Phosphatidylserine receptor Tim-4 is essential for the maintenance of the homeostatic state of resident peritoneal macrophages. Proceedings of the National Academy of Sciences 107, 8712–8717 (2010).

64. Vukmanovic-Stejic M et al. Enhancement of cutaneous immunity during ageing by blocking p38 MAPkinase induced inflammation. J Allergy Clin Immun (2017).

65. Jenner WJ & Gilroy DW Assessment of leukocyte trafficking in humans using the cantharidin blister model. JRSM cardiovascular disease 1, (2012).

66. Dinh PH et al. Validation of the cantharidin-induced skin blister as an in vivo model of inflammation. British journal of clinical pharmacology 72, 912–20 (2011). [PubMed: 21595743]

67. Watz H, Barnacle H, Hartley BF & Chan R Efficacy and safety of the p38 MAPK inhibitor losmapimod for patients with chronic obstructive pulmonary disease: a randomised, double-blind, placebo-controlled trial. Lancet Respir Medicine 2, 63–72 (2014).

68. Fehr S et al. Impact of p38 MAP Kinase Inhibitors on LPS-Induced Release of TNF-α in Whole Blood and Primary Cells from Different Species. Cell Physiol Biochem 36, 2237–2249 (2015). [PubMed: 26279429]

69. Pourcet B et al. LXRα Regulates Macrophage Arginase 1 Through PU.1 and Interferon Regulatory Factor 8. Circ Res 109, 492–501 (2011). [PubMed: 21757649]

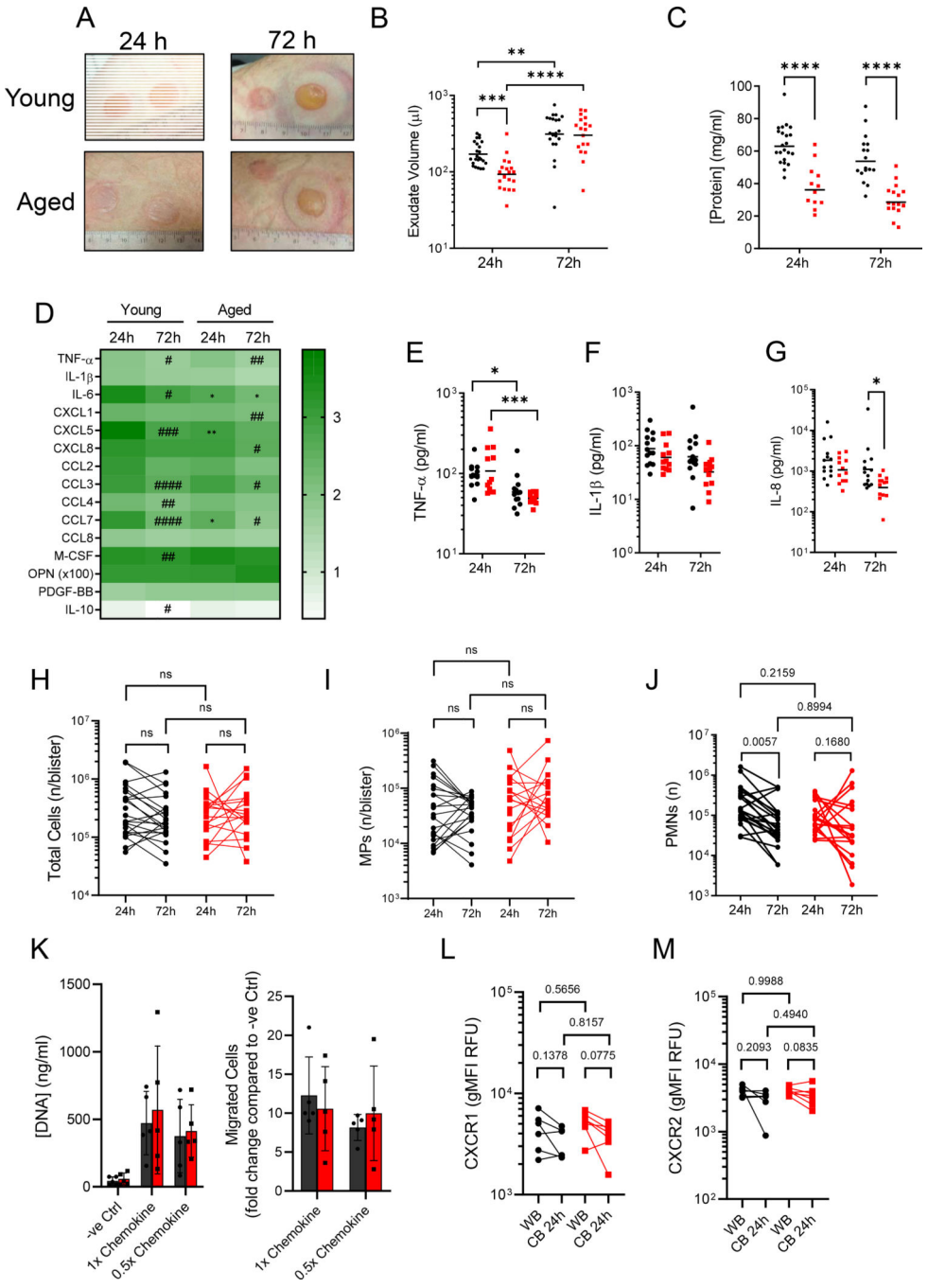

Figure 1: Cantharidin skin blisters reveal impaired neutrophil clearance in old humans.

A) Representative photographs of cantharidin skin blisters at 24 h and 72 h on young and aged participants. Ruler shows diameter in cm. **B)** Blister exudate volume determined by weight (n = 25 young, n = 22 aged). **C)** Total blister protein concentration determined by Bradford assay (n = 22 young at 24 h, 17 at 72 h. n = 12 aged at 24 h, 17 at 72 h.). **D)** Multiplex ELISA was used to quantify levels of 15 cytokines in cell-free cantharidin blister exudates and these are shown as a log-transformed heatmap (log[pgml]). # denotes temporal, within age-group differences per analyte, * denotes differences between age-groups for the

given time point (n = 13 young, n = 12 aged). **E)** TNF-α, **F)** IL-1β and **G)** IL-8 (CXCL8) (n = 13 young, n = 12 aged). **F)** Data are shown as a log-transformed heatmap of all 14 ELISA analytes in cell-free cantharidin blister exudate (log[pg/ml]). **H)** Total cell counts per blister determined by haemocytometer (n = 24 young, 20 aged). Polychromatic flow cytometry was performed to identify **I)** mononuclear phagocytes (MPs) and **J)** neutrophils (PMNs) in cantharidin blisters from young and aged volunteers at 24 h and 72 h (n = 22 young, 20 aged). **K)** 15 minute *in vitro* migration assays were performed on isolated peripheral blood PMNs. Flow cytometry was used to determine **L)** CXCR1 and **M)** CXCR2 expression on PMNs in peripheral blood (WB) and 24 hour cantharidin blister exudates. All plots show young in black and aged in red. Lognormally distributed data are plotted on a log scale, with the geometric mean. Normally distributed data are plotted on a linear scale with the arithmetic mean. For statistical analyses, lognormally distributed data were log-transformed. Each symbol represents a sample from a single participant. **B-M)** Two-way ANOVA with Sidak's multiple comparisons post-test correction. ns $p > 0.05$ * $p < 0.05$, ** $p < 0.01$ *** $p < 0.001$, **** $p < 0.0001$ or calculated p values values.

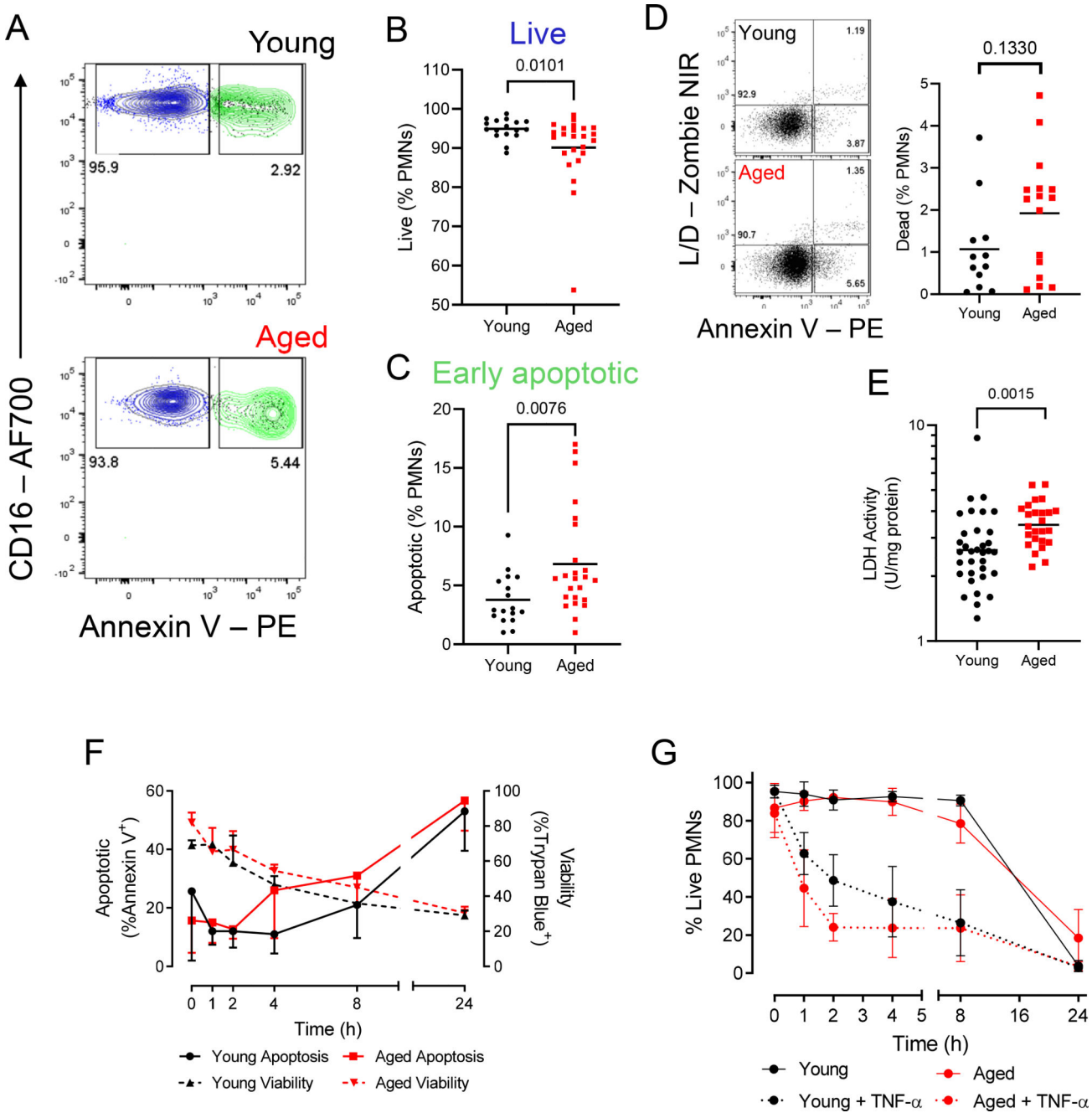

Figure 2: Apoptotic neutrophils accumulate in cantharidin skin blisters of the elderly, but apoptosis is unimpaired.

A) Representative dot plots for a young (top panel) and old (bottom panel) donor of a cantharidin skin blister sample at 24h, gated on Lin$^-$HLA-DR$^-$ cells, showing CD16 expression and Annexin V binding. **B)** Live CD16^{hi}Annexin V$^-$ cells and **C)** apoptotic, CD16^{hi}Annexin V$^+$ granulocytes are shown as a proportion of total granulocytes. Each symbol represents a sample from a single participant (n = 17 young, 24 old). **D)** Proportion of blister PMNs positive for a viability dye (n = 12 young, 16 old). **E)** Lactate dehydrogenase (LDH) measured in cell-free cantharidin blister exudate at 24 h (n = 34

young, 20 old). **B-D**) Mann-Whitney U test. **E)** Unpaired Student's *t* test with Welch's correction on log-transformed data. p values shown. **F)** Time-course of spontaneous *ex vivo* neutrophil apoptosis detected by annexin V binding (left y-axis, full lines) and death measured by a trypan blue viability stain (right y-axis, dotted lines). **G)** TNF-α inducible neutrophil apoptosis measured by cell viability over a 24 h time course. **F-G** show means and s.d. (n = 3 per group). Multiple unpaired *t* tests with Holm-Sidak correction. No significance ($p < 0.05$) detected.

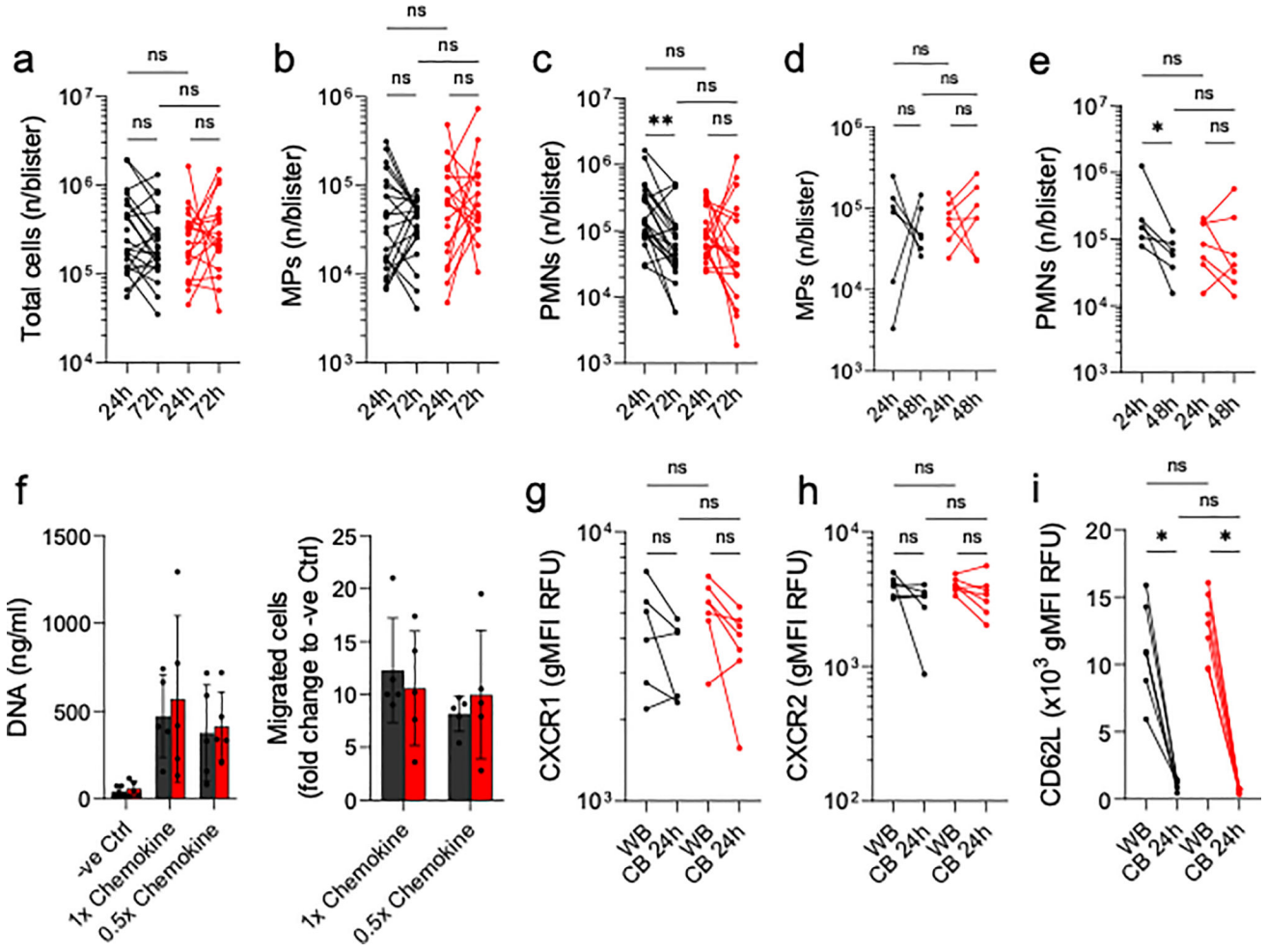

Figure 3: Efferocytosis is impaired in the elderly

Scatter plots for **A)** young (n = 21) and **B)** aged (n = 17) donor neutrophil clearance (expressed as 24 h – 72 h PMN numbers per blister) against 24 h MP infiltrates. Pearson correlations were carried out and a best-fit line with 95% confidence interval is given. **C)** Representative ImageStreamX images from an *ex vivo* efferocytosis assay using blister MPs (stained with CD14, red) and autologous, blood-derived apoptotic ACs (green) at a ratio of 5:1 ACs:MPs. Shown are images of a CFSE-stained apoptotic cell (AC), an AC-negative MP (MP), and MPs that have bound to an AC (<0) or that have ingested an AC (>0). Summary data of **D)** MPs that have associated with ACs (internal and external), **E)** the proportion of AC^+ MPs that have ingested their targets, **F)** the proportion of AC^+ MPs with bound-only ACs, and **G)** the overall proportion of MPs that have internalised ACs (n = 6 young, n = 5 aged). **H)** MPs were given ACs from young (Y AC) or aged (aged AC) donors and the overall efferocytic capacity was evaluated (n = 6). **I)** MP phagocytosis of ACs, opsonised latex beads (OLB) and naïve latex beads (LB) was compared using young and aged MPs. Phagocytosis of each target by young MPs was set to 100% (n = 3 young, n = 6 aged). **D-H)** Unpaired Student's *t* tests with Welch's correction. **I)** Two-way ANOVA with Sidak's multiple comparisons post-correction. * $p < 0.05$, ** $p < 0.01$, *** $p < 0.001$, **** $p < 0.0001$. # denotes significant differences within the aged cohort.

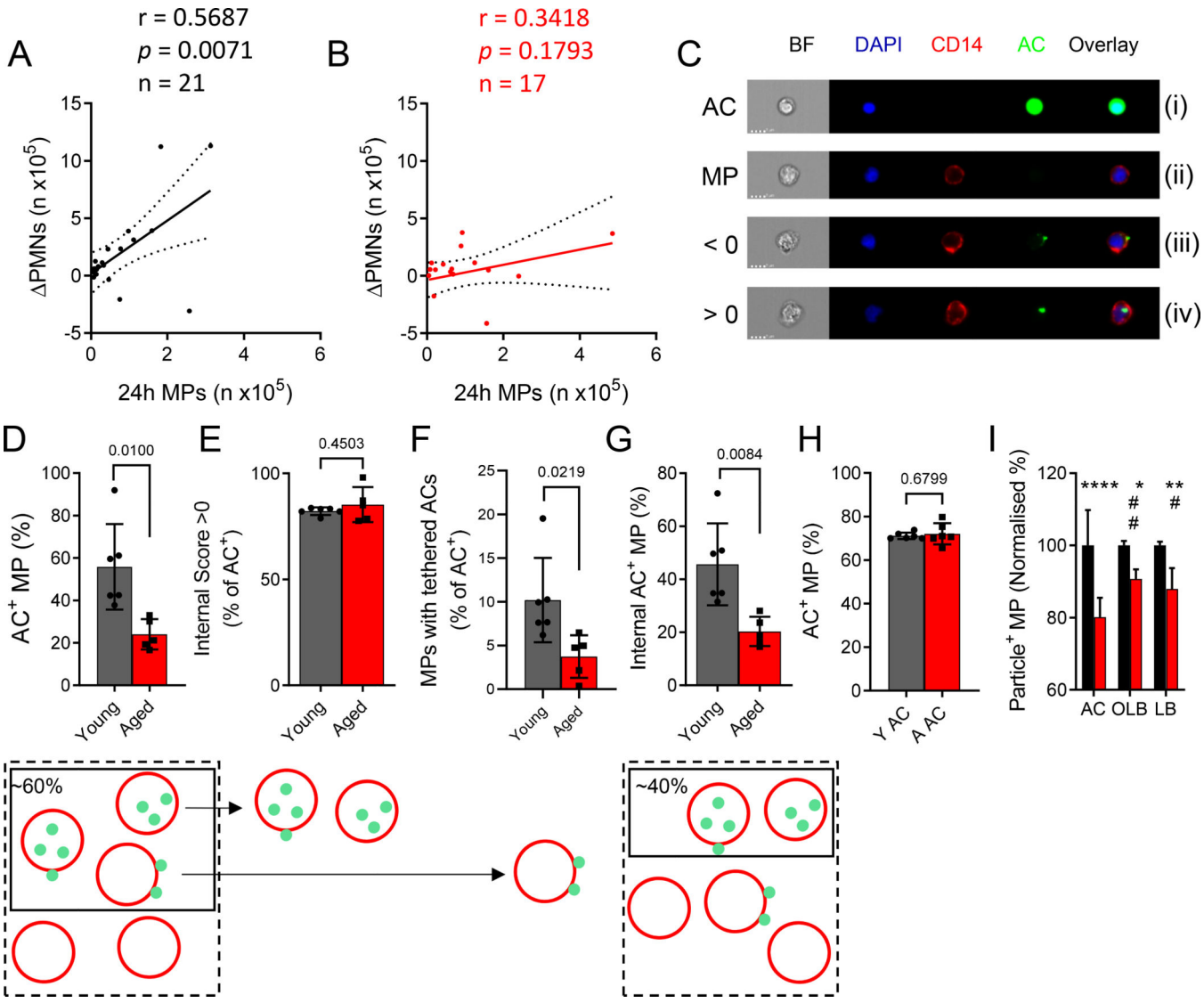

Figure 4: Reduced TIM-4 expression results in a failure to undergo resolution signalling in MPs from the elderly

Cell surface expression of **A)** MerTK and **B)** TIM-4 was determined by flow cytometry on MPs isolated from 24 h cantharidin blisters. For each marker, representative histograms are shown (grey: FMO control, black: young, red: aged). Summary data are shown on a logarithmic scale. Each symbol represents a single participant (n = 7 young, n = 11 aged). **C)** TIM-4 binding was inhibited using a polyclonal blocking antibody (5 μg/ml) and MP efferocytosis was compared between control and anti-TIM-4 (n = 3). Left y-axis shows overall AC^+ events, right y-axis shows internalization score. Imaging cytometry was used to determine nuclear translocation of **D)** NFκB (p65 subunit) and **E)** P-STAT3. Bright Detail Similarity (BDS) scores were calculated and untreated (ctrl) samples for each respective age group were set to 1 (n = 8 young, n = 4 aged). **F)** Cell surface expression of CCR7 was determined by flow cytometry on cantharidin blister MPs (n = 20 young, n = 14 aged). **G)** TGF-β levels in cell-free cantharidin blister exudates were measured by ELISA (n = 8 young, n = 9 aged). **H)** Blood-derived, cultured MPs were pre-treated with 10 μg/ml

polyclonal α-TIM-4 antibody or vehicle for 30 min before challenge with ACs (3:1) for 24 h. TGF-β levels were determined in cell-free culture supernatants (n = 3). **A-C** unpaired Student's *t* test. **D-E, H** Two-way ANOVA with Sidak's multiple comparisons post-correction. **F-G** Paired Student's *t* tests within age groups. * $p < 0.05$, ** $p < 0.01$, *** $p < 0.001$, **** $p < 0.0001$, or actual p values.

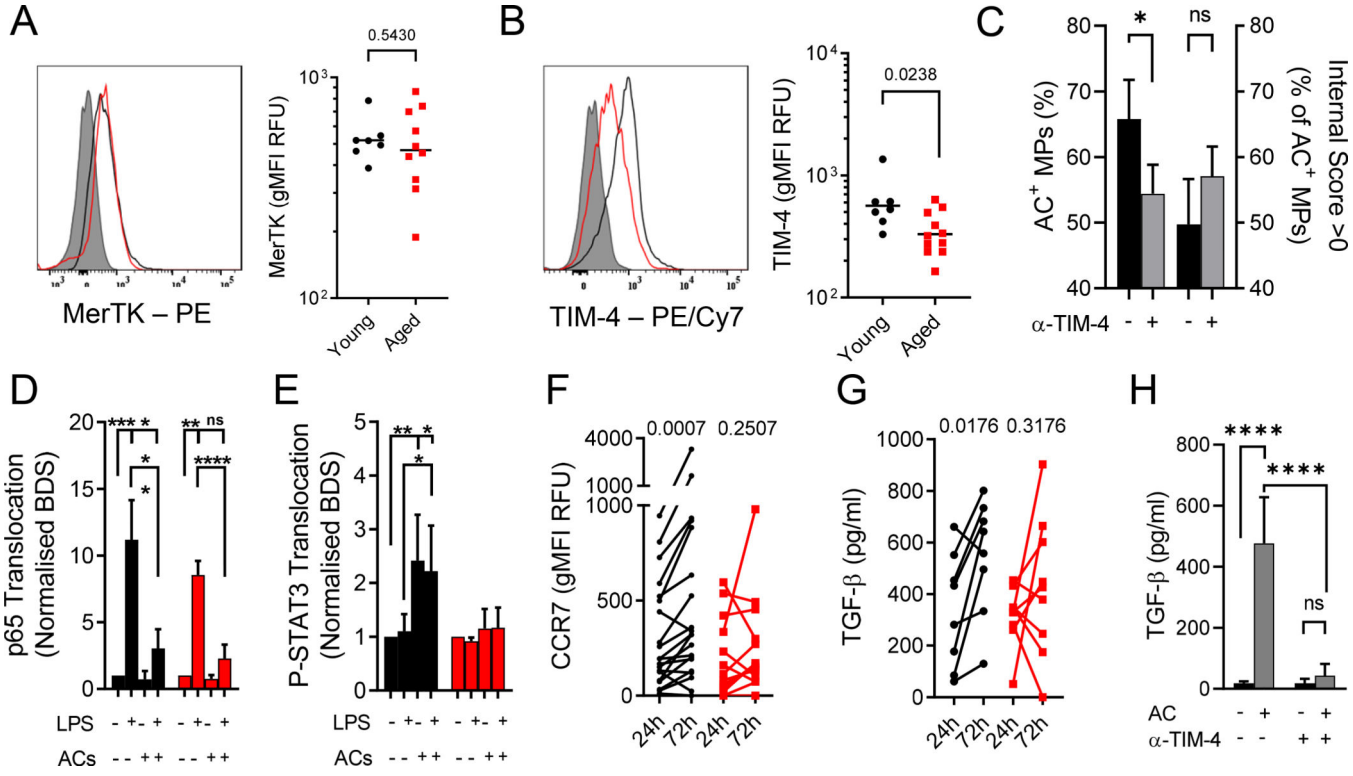

Figure 5: TIM-4 expression is regulated by p38 and p300.

Expression of TIM-4 was measured in young (black) and aged (red) donors by **A)** polychromatic flow cytometry on peripheral blood samples, gated on $CD14^{+}CD16^{-}$ monocytes, and **B)** qRT-PCR on isolated monocytes (n = 7 young, 4 old). **C)** Chromatin immunoprecipitation on isolated peripheral blood monocytes using antibodies against p300 and H3K27 acetylation marks. Two different sites, locations shown in the diagram, of the *tim4* promoter were amplified (n = 2 per group). **D)** Phosflow analysis of P-p38 expression in 24h cantharidin blister MPs and PMNs (n = 8 per group). **E)** Immunofluorescence of frozen, OCT-fixed whole skin sections obtained by punch biopsy (5 mm diameter). Sections were stained with P-p38 (green), CD163 (red), and DAPI (blue). Enumeration of **F)** total $CD163^{+}$ macrophages in naïve skin and **G)** the proportion of P-$p38^{+}$ macrophages (n = 9 young, 8 old). **H)** TIM-4 expression was assessed by flow cytometry on MPs cultured with 10 μg/ml LPS with and without 3 μM losmapimod over time (n = 3). **I)** Efferocytosis assay on MPs cultured for 72 h with or without losmapimod treatment (n = 7). **J-K)** MPs were treated with 10 μg/ml LPS with/without 3 μM losmapimod and the p300 inhibitors C646 and SGC-CBP30 (2.5 μM and 5 μM respectively). **J)** Chromatin immunoprecipitation using anti-H3K27Ac on cultured for 24 h (n = 2 pooled donors). **K)** Representative flow cytometry analysis of TIM-4 expression on MPs cultured for 72 h. Summary data of TIM-4, CD14 expression (left y-axis) and efferocytosis (right y-axis). Data were normalised to LPS alone for each donor (n = 5–8 per group). **A-B, D-G)** Unpaired Student's *t* test. **C**) Two-way ANOVA with Tukey's correction. **H-I**) Paired Student's *t* test. **K)** One-way ANOVA with Sidak's correction. Significance was tested with respect to LPS alone. * $p < 0.05$, ** $p < 0.01$.

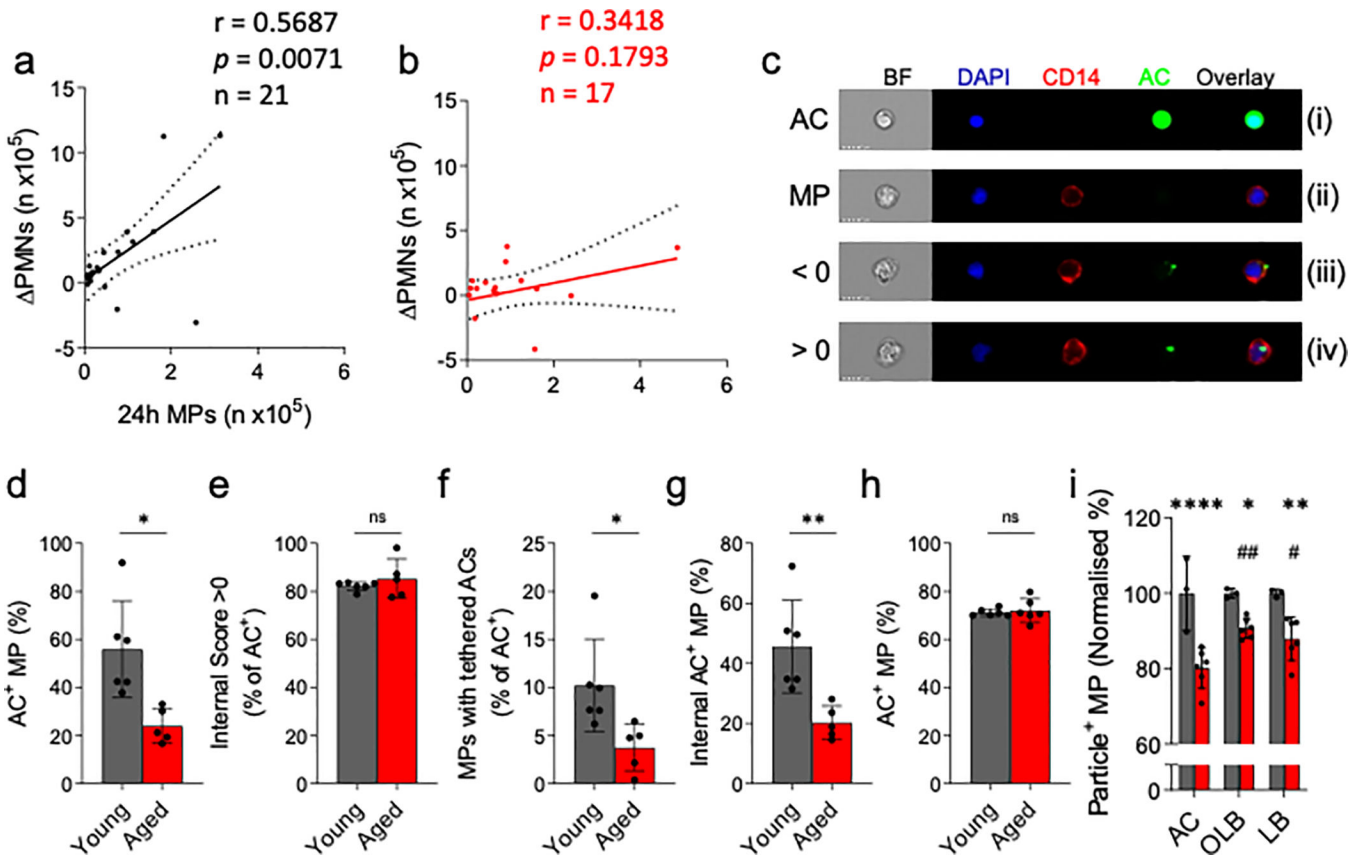

Figure 6: Blocking p38-driven inflamm-ageing in elderly humans restores inflammatory resolution.

A) The effects of losmapimod (15mg BID/PO for 4 days) on inflammation induced by topical application of cantharidin (0.1% w/v) to the skin were investigated in healthy old subjects (>65 years old, n=11, 6 female, 5 male). Levels of TNF-α in **B)** serum collected pre- and post-losmapimod treatment (n = 11), and **C)** 24 hour cell-free cantharidin blister exudates (n = 7) were measured by cytometric bead array. **D)** 24 hour cantharidin blister PMNs were enumerated by flow cytometry (n = 8). **E**) Representative dot plots for a cantharidin skin blister sample at 24h from an old subject without and with exposure to losmapimod gated on $Lin^{-}HLA\text{-}DR^{-}$ cells, showing CD16 expression and Annexin V binding; summary data are shown in the right-hand panel (n = 8). **F)** LDH activity levels in cell-free cantharidin blister exudates were measured by colorimetric assay (n = 9–34 per group, two-way ANOVA relative to the aged cohort. Holm-Sidak correction). Cell surface expression of **G)** TIM-4 and **H)** MerTK was determined by flow cytometry on MPs isolated from cantharidin blisters in the same subjects. (n=5). **I)** Scatter plots for young (n = 5, black), untreated aged (n = 9, red) and losmapimod-treated aged (n = 11, blue) donor neutrophil clearance (expressed as 24 h – 72 h PMN numbers per blister) against 24 h MP infiltrates. Pearson correlations were carried out and a best-fit line is given. **J**) Cell surface expression of CCR7 was determined by flow cytometry on cantharidin blister MPs from the same subjects exposed to cantharidin twice, once with and once without losmapimod (n=5). **K)** 72 h cell-free blister exudate levels of TGF-β were measured by ELISA (n = 5 per group). All plots show young in black, aged in red and aged+losmapimod in blue. **B-D**, **G-**

H, J-K) Two-tailed Student's *t* tests. **E)** Wilcoxon test. * $p < 0.05$, ** $p < 0.01$, *** $p <$ 0.001 or calculated p values.

Table 2.1:

Demographic data for the cantharidin blister characterisation study.

Age Group	**Young**	**Aged**	**Losmapimod**
Mean Age	27.7	74.9	77.3
Age SD	6.58	6.16	5.02
Recruited	24	21	11
Excluded	N/A	1	N/A
24h only	2/24	2/20	0/11
Gender (M/F)	8/16	9/11	5/6
Medication			
Antihypertensives	0	11	4
Anticoagulants	0	2	1
Miscellaneous†	4	1	1
HRT††	0	5	2

†Includes supplements, antidepressants and contraceptive pills.

††Includes tibolone and levothyroxine

Table 2.2:

List of antibodies used in flow cytometry.

Name	Supplier	Type	Clone
CD3	Biolegend	Mouse IgG2a	HIT3a
CD11b	Biolegend	Mouse IgG1	ICRF44
CD14	Biolegend	Mouse IgG2a	M5E2
CD14	Biolegend	Mouse IgG1	HCD14
CD16	Biolegend	Mouse IgG1	3G8
CD19	Biolegend	Mouse IgG1	HIB19
CD36	BD Biosciences	Mouse IgM	CB38 (NL07)
CD51 (ITGAV)	Miltenyi Biotec	Recombinant IgG1	REA181
CD56	Biolegend	Mouse IgG2a	MEM-188
CD62L	Biolegend	Mouse IgG1	DREG-56
CD66b	Biolegend	Mouse IgM	G10F5
CD95 (Fas)	Biolegend	Mouse IgG1	DX2
CD120a (TNFRI)	Miltenyi Biotec	Recombinant IgG1	REA252
CD120b (TNFRII)	Biolegend	Rat IgG2a	3G7A02
CD163	Biolegend	Mouse IgG1	RM3/1
CD181 (CXCR1)	Biolegend	Mouse IgG2b	8F1/CXCR1
CD182 (CXCR2)	Biolegend	Mouse IgG1	5E8/CXCR2
CD192 (CCR2)	BD Biosciences	Mouse IgG2a	LS132.1D9 (1D9)
CD197 (CCR7)	Biolegend	Mouse IgG2a	G043H7
CD206	Biolegend	Mouse IgG1	15-2
Siglec-8	Biolegend	Mouse IgG1	837535
HLA-DR	BD Biosciences	Mouse IgG2a	G46-6
MerTK	eBioscience	Rat IgG2a	DS5MMER
TIM-4	Biolegend	Mouse IgG1	9F4
P-p38	eBioscience	Mouse IgG2b	4NIT4KK
p65 (RelA)	Biolegend	Mouse IgG2b	14G10A21
P-STAT-3 (Tyr705)	Biolegend	Mouse IgG1	13A3-1
Live/Dead Zombie NIR	Biolegend	N/A	N/A

Table 2.3:

List of primers for ChIP and qPCR.

Gene	Application	Sequence (5'-3')
hChIP TIM4 seq 2 Fw2	ChIP	AGCCCACTTCTCAACTTCCT
hChIP TIM4 seq 2 Rv2	ChIP	ACAGGAATCCAGCAATGGGT
hChIP TIM4 seq 3 Fw3	ChIP	GCAGATATGGGCCAAAGGTG
hChIP TIM4 seq 3 Rv3	ChIP	CTGGGAAAGGGAATGGCTTT
hTim4 Fw1	mRNA	GTCCTCCCCAGTGATTCCTG
hTim4 Rv1	mRNA	CGTGGGATGTTGATGGGAGA
hCYPH Fw1	mRNA	TGTCTTTGGAACTTTGTCTGCAA
hCYPH Rv1	mRNA	GGCCGATGACGAGCCC